Title

Integrating Operator Information for Manual Grinding and Characterization of Process Performance Based on Operator Profile

Journal

Journal of Manufacturing Science and Engineering, 140(8)

ISSN

1087-1357

Authors

Das, Jayanti
Bales, Gregory L
Kong, Zhaodan
et al.

Publication Date

2018-08-01

DOI

10.1115/1.4040266

Peer reviewed

Integrating Operator Information for Manual Grinding and Characterization of Process Performance based on Operator Profile

Jayanti Das
Mechanical & Aerospace Eng.
University of California
Davis, California 95616
jydas@ucdavis.edu

Gregory L. Bales
Mechanical & Aerospace Eng.
University of California
Davis, California 95616
glbales@ucdavis.edu
ASME Member

Zhaodan Kong
Mechanical & Aerospace Eng.
University of California
Davis, California 95616
zdkong@ucdavis.edu
ASME Member

Barbara Linke
Mechanical & Aerospace Eng.
University of California
Davis, California 95616
bslinke@ucdavis.edu
ASME Member

ABSTRACT

Due to its high versatility and scalability, manual grinding is an important and widely used technology in production for rework, repair, deburring, and finishing of large or unique parts. To make the process more interactive and reliable, manual grinding needs to incorporate ‘skill-based design’ which models a person-based system and can go significantly beyond the considerations of traditional human factors and ergonomics to encompass both processing parameters (e.g., feed

rate, tool path, applied forces, material removal rate) and machined surface quality (e.g., surface roughness). This study quantitatively analyzes the characteristics of complex techniques involved in manual operations. A series of experiments have been conducted using subjects of different levels of skill, while analyzing their visual gaze, cutting force, tool path, and workpiece quality. Analysis of Variance (ANOVA) and multivariate regression analysis were performed and showed that the unique behavior of the operator affects the process performance measures of specific energy consumption and material removal rate. In the future, these findings can be used to predict product quality and instruct new practitioners.

Keywords

Human factors, grinding, surface roughness, processing parameters, forces, gaze behavior, operator's experience

1. Introduction

In the age of Industry 4.0, manufacturing can be described as a 5M system, which consists of Materials (properties and functions), Machines (precision and capabilities), Methods (efficiency and productivity), Measurements (sensing and improvement), and Modeling (prediction, optimization, and prevention) [1]. With recent development and an ever-growing use of sensors, data acquisition systems, and real-time learning algorithms, cyber-manufacturing systems have been able to transform raw data into meaningful and actionable operations. Yet despite the adoption and proliferation of automation, human skill and flexibility remain an integral part of many operations. Manual abrasive finishing is widely used in industry. These processes include deburring, engraving, weld grinding and polishing in the aerospace, construction and welding industries [2]. Unfortunately, these manual procedures are heavily dependent on the skill of the operator in retrieving, organizing, and processing information. Therefore, humans are not merely

the supervisors of production operations, but also performers of these manual tasks. A skilled operator is expected to be highly adaptable, flexible, and able to quickly learn from process changes. Studies have shown that skills involved in these manual tasks are largely procedural rather than declarative, meaning that they are self-regulatory and orchestrated by an individual operator [3, 4]. Surprisingly, even though manual abrasive operations have a growing market, they are under-researched, and limited work has been done on manual process parameters and their effect on surface integrity. Therefore, there exists an opportunity to improve human-machine interaction and facilitate the growth of the cyber-manufacturing infrastructure into areas where automation is not likely. To increase support from such cyber systems, human behavior must be effectively quantified and predicted.

Unlike automated processes in which cutting tools follow a guided path at a constant velocity (‘path-control’), manual machining operations are ‘force controlled.’ Rather than a ‘constant feed rate,' manual feed (Fig. 1) is provided by the individual operator and is critically dependent on posture, motion, gripping forces, and body forces. Manual feed causes cutting-force variations on the workpiece in all three directions (tangential, normal, and axial) as shown in Fig. 1. These 3D force variations influence surface quality (e.g., surface roughness, shininess, etc.). Unfortunately, there is no quantitative data available in the literature regarding the impact of these force variations on surface integrity based on operator profile.

A detailed investigation of the interrelationship between skill level and process performance can quantify the intricate behavioral complexity involved in manual operations. It can be anticipated that for manual operations, machining process parameters are largely dependent on human-machine interactions [4] and can greatly influence product outcome [5, 6]. To make this human-machine interaction more effective, there is a need for a quantified, formal method of measuring,

representing, transferring, and reasoning about human skills in order to (i) efficiently allocate resources and tasks among humans, between humans and machines, and cross-factories, (ii) expand and enhance human capabilities, and (iii) optimize system behavior to predict the product performance. A lack of understanding of these manual skills may prolong the transfer of knowledge among generations of workers and critically impact technological development, in the form of devices, interfaces, or procedures that can enhance human capabilities.

The broader scope of this research is to develop a smart analytics system for manual grinding which can transform experience-based knowledge into evidence-based decision-making for sustainable operations and reliable product performance. This study focuses on understanding the visual-attention-motor behavior [3] of differently skilled workers to gain scientific knowledge for reasoning operation and product quality. This paper presents a study in which input-output streams of manual grinding operations are discussed, and a comparative study of product performance is evaluated in terms of user's skill level and cutting forces coming from manual feed. To find the correlation between applied force variation and part performance, this study additionally investigates the sensorimotor behaviors of visual gaze, and tool paths during the performance of a manual grinding task.

2. Factors Involved in Manual Operations

To find the right balance between attaining reliable product performance and maximizing process efficiency is complex and depends on a number of processing factors. The 3D cutting forces shown in Fig. 1, are critically dependent on the motor behavior of the individual operator. Workpiece quality can vary highly based upon the worker's skills, which include posture, motion, gripping forces, and applied tool path. A poor control of these processes negatively impacts the geometrical and physical properties of the surface, which ultimately affect part

functionality [7]. In this study, part functionality was evaluated by measuring different types of surface roughness parameters [8].

A comprehensive input-output diagram, shown in Fig. 2, helps to elucidate the resource streams of the process. The color code used in this diagram is similar to the general grinding resource streams reported in [9]. In addition to the resource streams, the process is affected by the worker, the machine and the environment. As depicted in Fig. 2, processing energy, surface texture, abrasive materials composition, and the social aspects of workers (e.g., health, education) can directly or indirectly impact the finished product and determine the nature of waste. These process-flow diagrams often help in choosing appropriate sustainability indicators [10]. For example, this diagram can direct web-based tools, on-board sensing technology, and wireless communication to map out the transformation processes occurring within the input-output stream. Recently the ASTM International E60.13 subcommittee on sustainable manufacturing initiated a standard structure to formally characterize manufacturing processes, which enables the seamless sharing and use of manufacturing information [11]. This repository model motivates the ubiquitous and extended use of a standardized representation of unit manufacturing processes (UMPs) across industries and can help to provide a tangible, data-driven perspective for modern manufacturing.

The objective of this repository model is to identify which parameters influence process physics to potentially improve manufacturing practices, including energy consumption minimization, and material flow control throughout the production scenario. Fig. 3 shows the graphical representation of a UMP model, composed of five information flows:

Inputs: This section provides information on material/energy flows into the manufacturing process. Apart from processing energy, workpiece material, and tool geometry, for manual

operation the grinding forces are a function of operator's technical skill-level and manual feed rate.

Product and Process Information: This section provides all control parameters associated with cutting tool speed, equivalent chip thickness, specific removal rate, generated surface roughness, etc.

Resources: This section provides information about tooling and equipment requirements. In this study, four subjects used a Dremel 4000 handheld tool. Detailed information is provided in Fig. 3.

Transformation: This is the important section containing rules, equations, and an association of uncertainty related to input and control parameters with the output.

Outputs: This section illustrates the association of inputs, transformation on machined product, and generated waste, from the process interaction. For manual operation, the material removal rate and final surface roughness becomes a function of the grinding forces.

3. Experimental Method

3.1 Experimental Setup

To study the impact of an operator's skill on process outputs, we have chosen four subjects with various level of proficiency. Here we defined skill as the efficient techniques applied by operators to produce reliable part quality with the grinding tool. Four subjects were defined as Subject 1, 2, 3, and 4; where Subject 1 is very efficient to produce kitchen knives in small scale using manual grinding. Subject 2 and Subject 3 have been involved with grinding tasks in the last 2-3 years to produce reliable workpieces confirmed by confocal microscopy and Subject 4 has limited grinding experience. Additional information was gathered from each subject via initial questionnaire (i.e., age, occupation, fitness level, the presence of any related health issues, etc).

Subject 1	Has good amount of exposure with manual grinding to produce reliable product quality
Subject 2	Spent 2-3 years with manual grinding tools to produce reliable products
Subject 3	Spent 2-3 years with manual grinding tools to produce reliable products
Subject 4	Has limited experience but received basic training to perform manual grinding operation

Each test coupon contained light scratch marks in the vertical plane throughout the surface. The subjects were asked to remove the marks using a Dremel 4000 grinding power tool. As shown in Fig. 4, four streams of data were collected. First, the direction of gaze was measured using an eye tracking system. Second, triaxial grinding forces (axial, tangential, normal) were measured using a Kistler piezoelectric force sensor (model 9251A) with a sampling rate of 1000 Hz. Third, an Optitrack motion tracking system was used to capture the kinematic motion of the tool path. Finally, the topographical features of the finished surface (3D surface roughness, surface isotropy) were analyzed using confocal scanning microscopy (model Zeiss Axio CSM 700). All topographical data were measured under 10x magnification with a cut-off length of 0.8 mm and an evaluation length of 4 mm (in accordance with ISO 4287:1997). A 7 x 7 stitching method was applied for maximum coverage of sample surfaces.

The Optitrack motion tracking system consists of 12 wall-mounted cameras, each of which contain a ring of infrared light emitting diodes that project into the tracking area. The grinding tool was marked with reflective spheres to provide 6 degree of freedom pose estimation to <1mm accuracy (Fig. 4). This data was sampled at 120 Hz. The visual behavior of each subject was measured using a wearable eye-tracking system manufactured by SensoMotoric Instruments (Model SMI ETG 2w), which is integrated into a set of glasses and can extract binocular gaze while simultaneously recording a video of the visual point of view. Gaze data was sampled at 60 Hz.

3.2 Surface Preparation

The material used in this study was 6061 aluminum in the form of test coupons with dimensions of 50 mm in length, by 25 mm in width, by 25 mm in height. Each grinding experiment was conducted with a Dremel 4000 hand-held power tool using 6.35 mm diameter alumina sanding

bands of grit size 60 (mesh number) with a cutting speed of 3.32 m/s. The power tool was run at a constant speed of 5000 rpm. All grinding operations were performed under dry cutting conditions. Each subject repeated ten trials with a new abrasive sanding band for each trial. In the grinding experiment, no crossfeed was provided, neither any surface treatment conducted after grinding

4. Results & Discussion

4.1 Process Monitoring and Workpiece Properties based on Operator Profile

The forces applied by the operator cause abrasive grains to penetrate the workpiece and it is the variation in this grain-surface interaction that influence surface quality [12]. The increase in grain penetration depth affect the three main stages of material removal: rubbing, plowing, and cutting. Deep penetration causes material removal (cutting), penetration without material removal causes plowing, while small penetration (rubbing) results in mild tool wear [13]. However, all three stages can simultaneously occur [14, 15]. Many aspects of grinding behavior depend on this material removal process and can directly influence workpiece quality - thus becoming a function of applied forces [9, 16, 17].

Fig. 5 illustrates the average tangential and normal forces for all trials. The figure shows that Subject 1 was highly consistent with the lowest inter-trial variance, whereas, Subject 4 has high variability. Among all four subjects, Subject 2 and Subject 4 applied higher tangential and normal forces. Overall, tangential forces were higher compare to normal forces, and axial forces were negligible and thus ignored from further analysis.

Time-series profiles of the acquired force data reveal that the cutting forces have a direct impact on the surface generation and material removal rate (MRR). Fig. 6 shows that Subject 2 and

Subject 4 exhibited higher cutting forces and higher average roughness compared to Subject 1 and Subject 3. Overall, Fig. 6 highlights that with increasing cutting force, surface roughness increases while MRR decreases. Generally, higher forces cause vibration and chatter during the grinding process, which inevitably worsen the quality of finished surface. The data depicted in Fig. 6 have been "standardized" via dividing by their standard deviations to ensure comparability.

Material removal rate (MRR) is a useful parameter to understand the cutting mechanisms. For high MMR, chip formation dominates whereas in lower MMR, rubbing and plowing prevail. Since energy is lost to heat conversion during all phases, higher proportions of chip formation lead to a more effective grinding process. Subject 1 and Subject 3 (Fig. 6.) showed higher MRR and lower cutting forces compared to Subject 2 and Subject 4, and presumably cut more effectively. In addition, higher grinding forces accelerate tool wear, and a sufficiently high force can lead to separation of the grit from the abrasive wheel. Furthermore, high forces reduce workpiece integrity and shorten tool life [9]. Therefore, lower grinding forces with higher material removal rates (as shown by Subject 1 and Subject 3 in Fig. 6) are desirable. Since tool life is an important factor in the overall operational cost, cutting forces have a direct influence on the overall grinding expenditures [18].

4.2 Tool Path

The motion tracking system allows the dynamic measurement of tool position. Fig. 7 compares the distinct tool paths for each subject. To improve visualization, only 75% of a single trail period is shown. This method helps to capture the detailed techniques utilized by operators of different levels of skill level.

All four subjects show unique tool path behavior. Subject 1 and Subject 3 have moved the tool in the complex path, which is a combination of side-to-side and swirling motion. Subject 2 and Subject 4 have shown simple side-to-side motion. However, Subject 4 covers only a small portion of workpiece leaving many areas untouched.

An analysis of performance shows that Subject 1 and Subject 3 produce a higher surface quality. This was accompanied by distinct differences in their gaze and motor behavior. We have referred to these sets of behavioral patterns as the exhibition of a technique. For ease of syntax, Subject 1 and Subject 3 show a more complex tool path behavior and we have referred this as Technique A while Subject 2 and Subject 4 utilize Technique B. The behaviors associated with these techniques have been summarized in Table 1. Table 1 also shows that Subject 1 and Subject 3 were able to remove more mass in a shorter period while utilizing lower normal and tangential forces, with lower gaze frequency, and lower gaze shifts compared to Subject 2 and Subject 4. Furthermore, Subject 1 and Subject 3 have greater axial tool velocity and lower isotropy which results in higher average surface roughness. The detail of gaze frequency and gaze shifts have been discussed in [4], so Table 1 only summarizes the overall distinct behavioral differences. The quantitative information of these behavioral differences is shown in Table 2.

The quantitative findings from Table 2 can be summarized as follows:

1. The tangential RMS tool velocity is 24% lower for Technique A than for Technique B.
2. The mean gaze frequency is 48% higher for Technique A than for Technique B.
3. The axial RMS gaze shifts are 26% higher for Technique A than for Technique B.
4. The mean tangential force is 27% lower for Technique A than for Technique B.
5. Mean machined surface isotropy is 41% lower for Technique A than for Technique B.

6. Mean processing time is 13% lower for Technique A thank for Technique B.

Analysis of the tool path data was performed to compare the motion characteristics between the individual techniques. These behaviors can change abruptly or slowly as the task progresses, so we cannot assume that the time series is stationary over the course of a single grinding trial. It is reasonable however, to assume minimal changes in motor behaviors over relatively short timescales. Therefore, we have sectioned the time series data into a sequence of 1 second segments over which we do assume stationarity. Given the data show in Fig. 7, we would expect to see roughly 2-3 sweeps of the tool.

Each subject has the ability to maneuver the tool in the axial and tangential directions independently. The separate degrees of freedom are only linked via purposeful movement, and any detectable coupling between the two would be an indication of their deliberate technique. In order to capture this relationship, we use a first order, multivariable autoregressive model, AR(1). The general expression for an AR(1) system is given by:

$$x_i = Ax_{i-1} + w + \epsilon_i \tag{1}$$

where $x_i \in \mathbb{R}^N$ is a vector of measurements at the i^{th} time step, $A \in \mathbb{R}^{N\times N}$ is the coefficient matrix for the AR(1) model, $w \in \mathbb{R}^N$ is the intercept vector or bias, and $\epsilon_i \in \mathbb{R}^N$ are independent, identically distributed (iid), Gaussian white noise terms with zero mean and covariance Σ. If we center each of the segments about its mean, the bias term is effectively zero and, we can express our AR(1) model for our two degree of freedom system as

$$\begin{bmatrix} X_i^T \\ X_i^A \end{bmatrix} = \begin{bmatrix} a_{11} & a_{12} \\ a_{21} & a_{22} \end{bmatrix} \begin{bmatrix} X_{i-1}^T \\ X_{i-1}^A \end{bmatrix} + \begin{bmatrix} \epsilon_i^T \\ \epsilon_i^A \end{bmatrix}. \tag{2}$$

Here X_i^T is the tangential position and X_i^A is the axial position. Given the iid noise terms, we can approximate the A matrix using stepwise, least squares estimation and solve the system for the current axial position X_i^A as a function of the past X_{i-1}^A and X_{i-1}^T.

$$X_i^A = \left(\frac{a_{21}}{a_{11}}\right) X_{i-1}^T + \det(\mathrm{A}) X_{i-1}^A \tag{3}$$

If we let $\alpha = \left(\frac{a_{21}}{a_{11}}\right)$ and $\beta = \det(A)$, we obtain a parametric expression for the axial/tangential coupling.

Fig. 8 displays the α and β values for each of the four subjects. We can see that the data is concentrated tightly about β=1. The AR model assumes that the system is causal and stable, comprised of an independent and a dependent variable. In this framework, we would expect that the current value of the axial position would depend little upon its past value and a β value of unity enforces that notion. In contrast, the α values describes how the current value of the axial position depends on the past value of the tangential position, or more specifically, the swirling motion of the tool. Large negative values of α correspond to very tall (axial), counterclockwise, oval shaped tool paths where small values correspond to wide (tangentially) ones.

Fig. 9 plots the normalized histograms of the α parameter for all four subjects and illustrates how each of the subjects utilize the swirling technique. From Fig. 9 it is clear that Subject 2 performs the task primarily with sweeping tangential, and very slows vertical motions across the sample. By contrast, Subjects 2 and 4 both utilize more circular movements, each with different eccentricities; Subject 4 exhibiting taller (axial) orbits than the Subject 4. Finally, while Subject 1 spends much of the time performing motions very similar to Subject 2, the tail of the distribution moves far to the left indicating the use of a very wide range of orbital eccentricities,

both wide and tall. In fact, Subject 1 displayed an exceptionally wide range of tool path behavior, from primarily axial, to primarily tangential, and everything in between.

4.3 Specific Energy Consumption and Process Performance

The specific grinding energy (e_c) is the energy per unit volume of material removed. It can be expressed as following, where F_t is the tangential forces, v_s is the rotational cutting tool velocity and Q_w is the material removal rate.

$$e_c = \frac{F_t v_s}{Q_w} \tag{4}$$

Fig. 10 represents the specific energy (e_c) consumption versus the material removal rate (Q_w) for four subjects. It is one of the most important parameters to assess grinding performance and is critically dependent on the workpiece material and grinding conditions. Specific energy is composed of the energy for rubbing and plowing material, forming grinding chips, as well as overcoming friction between the grinding grits, the tool bond, and the workpiece. Generally, for a highly effective grinding process, the friction energy is assumed to be negligible. Therefore, the overall specific energy can be expressed as follows:

Specific Energy (e_c) = Rubbing Energy + Plowing Energy + Cutting Energy (Chip Formation Energy)

A low MMR implies that a significant amount of energy is consumed from rubbing and plowing rather than cutting, whereas a higher MMR indicates that energy is consumed for chip formation [19]. Fig 10 shows that under low MRR the process consumes a higher amount of energy. This energy consumption gradually decreases with increasing MRR. Under the same grinding conditions, Subject 4 exhibits the highest specific energy consumption whereas Subject 1 displays the lowest. Large specific grinding energy is undesirable because it results in high-

energy consumption and a high cost of material removal [20]. The higher removal rate is beneficial to reducing cutting energy. Subject 1 shows efficient cutting behavior with a minimum of specific energy consumption and only a 48% variation in MMR.

4.4 Signal to Noise Ratio based on Operator Profile

Fig. 11 represents the results of the signal to noise ratio (S/N ratio) for four process parameters at three levels (minimum, maximum, mean). Here the term 'signal' represents a desirable value (in this case roughness) whereas, the 'noise' represents the standard deviation (undesirable value). Hence the S/N ratio represents the amount of variation present in the quality characteristics [21]. Depending on the purposes and applications, different types of S/N ratios exist [22]. Here the desirable objectives are to lower the cutting forces and the surface roughness. Therefore, the lower-the-better type S/N ratio was applied to transform the observed data as follows:

$$\eta = -10log_{10} \sum_{i-1}^{n} y_i \quad (5)$$

Here η is the S/N ratio for the lower-the-better case, y_i is the measured quality characteristic for i^{th} repetition, and n is the number of repetitions for a trial. The S/N ratios for four process parameters (tangential and normal forces, depth of cut, and processing time) at three levels for achieving lower surface average roughness is tabulated in Table. 3.

Fig. 11 shows that, for Subject 1, lower surface roughness was obtained at a 4 N tangential force (level 1), a 0.25 N normal force (level 1), a 0.13 μm depth of cut (level 2), and a processing time of 64 sec (level 1). For Subject 1, the average surface roughness decreased with increasing tangential force. Subject 3 showed an increase of average surface roughness with decreasing normal force, tangential force, and processing time, and with increasing depth of cut. Subject 2 showed an increase of average surface roughness with increasing processing time. In contrast,

Subject 4 showed no particular pattern due to the inconsistent performance from trial to trial. From S/N ratio, it is possible to find the most effective parameters that influence process results. We can determine the optimal sets of process parameters from the main effects plot for S/N ratio shown in Fig 11.

4.5 Statistical Analysis

Analysis of Variance (ANOVA) is a computational technique to estimate the relative contribution of each controlled parameter to the overall response quantitatively and is expressed in percentage. In our study, ANOVA was used to understand a detailed visualization of the impact of independent processing parameters on average surface roughness based on two the distinct techniques discussed in this study (i.e., **Technique A and Technique B**) during manual grinding. This study helped quantify and analyze the contribution and comparative significance of each independent processing parameter to predict the outcome. Statistical analyses were performed using Stata 14 software (StataCorp LP). Linear regression and Analysis of Variance (ANOVA) were performed following log base-10 transformations of standardized surface average roughness. Tukey's HSD (honest significant difference) and Wald's test for linear hypothesis were used for post-hoc comparisons between treatment levels. Significance (α) for all analyses was set at ≤ 0.05. The analysis was carried out at the level of 95% confidence interval, and results were shown in Table. 4. The column of contribution from Table. 4 showed the percentage impact of each parameter on the total variation, signifying the degree of effect on the results. The larger the percentage contribution, the greater the influence of a parameter on surface roughness.

The regression model consisted of a set of four predictors: tangential and normal force, depth of cut, and processing temperature. The degree of freedom is always same as the number of predictors, which are four for this model. The model was based on log base-10 transformation as per the requirement of a normally distributed outcome variable. Based on the analysis, our hypothesis is, the surface roughness of independent variable, Subject 1 & 3 and Subject 2 & 4 are significantly different when using Technique A & B respectively.

H_0: $\mu_{TechniqueA} \neq \mu_{TechniqueB}$

H_1: H_0 is rejected

Predictive model equations for Techniques A and B are shown below in equations (6) and (7). This estimated value or predictive model expresses how surface roughness changes for a unit change of the predictor values.

Predictive Model for Technique A (Subject 1 & Subject 3)

$$log_{10}(R_a) = 1.78 + 0.02F_T - 0.77F_N + 0.22a_e - 0.01t_p \quad (6)$$

Predictive Model for Technique B (Subject 2 & Subject 4)

$$log_{10}(R_a) = 1.51 + 0.01F_T - 0.42F_N - 0.57a_e - 0.001t_p \quad (7)$$

Equation (6) and equation (7) agree with our findings from Fig 6. For a complex tool path, and a technique, which consists of greater axial tool velocity, higher gaze frequency, larger axial gaze shifts, and lower tangential force, surface isotropy, and processing time; tangential force and depth of cut show a positive association with the product outcome. From equation **(6)**, it can be predicted that for a unit change of tangential forces, normal forces, depth of cut, and processing time; the average roughness might increase 1.05 μm, decrease 5.89 μm, increase 1.66 μm, and

decrease 1.02 μm respectively. Whereas, for a simple tool path, and a technique consisting of lower axial tool velocity, lower gaze frequency, larger tangential gaze shifts, and higher surface isotropy, and processing time; normal force and depth of cut show a negative association with the product outcome. From the equation **(7)**, it can be predicted that for a unit change of tangential forces, normal forces, depth of cut, and processing time; the average roughness might increase 1.02 μm, decrease 2.63 μm, decrease 3.72 μm, and increase 1 μm respectively. Both equations show that irrespective of the machining technique, surface roughness decreases with increasing the normal forces. This pilot study has shown that there are observable and distinguishable sensorimotor behaviors associated with two distinct techniques utilized by the individual subjects, and more importantly, that task performance is affected by these techniques. Certainly, an experiment with a larger cohort of subjects representing each experience level would be required in future work.

Conclusion

A new experimental setup was used in this study to monitor human skills during manual grinding operations. The experimental observation integrates operator's information (i.e. techniques, applied forces, processing time, material removal rate, tool path) and characterizes process performance in the surface roughness based on operator profile. Our results show that operators' inherent techniques control machining performance along with experience level. Statistical analyses were carried out to develop a predictive model based on unique the behavior associated with operator's skill level. By comparing data obtained from subjects with different levels of skill, we are able to quantitatively associate characteristics of human manual skill and process performance (i.e., specific energy consumption, material removal rate, etc.).

The limitations of these operator-based models are primarily the limited sample sizes and the subjective declaration of operator's skill-level. Standardizing the range of operator's skills, techniques, and increasing the sample sizes can significantly improve the model for these sort of data-driven analyses and will help to predict the outcome more accurately.

This study, on the one hand, improves understanding of complex manual skills thus paving the road for the improved preservation and transfer of knowledge, and on the other provides the scientific and empirical underpinnings for the future development of robotic devices and computer interfaces for augmenting manual operations.

Acknowledgement

The authors want to thank the Engineering Fabrication Laboratory (EFL) and Advanced Materials Characterization and Testing (AMCaT) facilities of the University of California Davis for the use of their machine equipment and confocal microscope facilities. The authors express their sincere thanks to Prof. Dr.-Ing. Jörg Seewig, Professor of the University of Kaiserslautern, Germany for his extended cooperation. This research did not receive any specific grant from funding agencies in the public, commercial, or not-for-profit sectors.

References

[1] Lee, J., Lapira, E., Bagheri, B., and Kao, H.-a., 2013, "Recent advances and trends in predictive manufacturing systems in big data environment," Manufacturing Letters, 1(1), pp. 38-41.
[2] Goldstein, E. B., 2014, Cognitive psychology: Connecting mind, research and everyday experience, Nelson Education.
[3] Bales, G., Das, J., Linke, B., and Kong, Z., 2016, "Recognizing Gaze-Motor Behavioral Patterns in Manual Grinding Tasks," Procedia Manufacturing, 5, pp. 106-121.
[4] Bales, G. L., Das, J., Tsugawa, J., Linke, B., and Kong, Z., 2017, "Digitalization of Human Operations in the Age of Cyber Manufacturing: Sensorimotor Analysis of Manual Grinding Performance," Journal of Manufacturing Science and Engineering, 139(10), pp. 101011-101011-101018.

[5] Francalanza, E., Borg, J., and Constantinescu, C., 2017, "Development and evaluation of a knowledge-based decision-making approach for designing changeable manufacturing systems," CIRP Journal of Manufacturing Science and Technology, 16, pp. 81-101.
[6] Lee, J., Bagheri, B., and Kao, H.-A., 2015, "A cyber-physical systems architecture for industry 4.0-based manufacturing systems," Manufacturing Letters, 3, pp. 18-23.
[7] Davim, J. P., 2010, Surface integrity in machining, Springer.
[8] Das, J., and Linke, B., 2017, "Evaluation and systematic selection of significant multi-scale surface roughness parameters (SRPs) as process monitoring index," Journal of Materials Processing Technology.
[9] Aurich, J. C., Linke, B., Hauschild, M., Carrella, M., and Kirsch, B., 2013, "Sustainability of abrasive processes," CIRP Annals - Manufacturing Technology, 62(2), pp. 653-672.
[10] Gibson, K., and Tierney, J. M., 2011, "The evolution of environmental management systems: Back to basics," Environmental Quality Management, 21(1), pp. 23-37.
[11] Bernstein, W. Z., Mani, M., Lyons, K., Morris, K., and Johansson, B., 2016, "An Open web-based repository for capturing manufacturing process information," ASME 2016 international design engineering technical conferences and computers and information in engineering conference.
[12] Khellouki, A., Rech, J., and Zahouani, H., 2007, "The effect of abrasive grain's wear and contact conditions on surface texture in belt finishing," Wear, 263(1), pp. 81-87.
[13] Klocke, F., and Linke, B., 2008, "Mechanisms in the generation of grinding wheel topography by dressing," Production Engineering, 2(2), pp. 157-163.
[14] Tönshoff, H. K., Peters, J., Inasaki, I., and Paul, T., 1992, "Modelling and Simulation of Grinding Processes," CIRP Annals - Manufacturing Technology, 41(2), pp. 677-688.
[15] Linke, B., Duscha, M., Klocke, F., and Dornfeld, D., 2011, "Combination of Speed Stroke Grinding and High Speed Grinding with Regard to Sustainability."
[16] Malkin, S., and Guo, C., 2008, Grinding technology: theory and application of machining with abrasives, Industrial Press Inc.
[17] Marinescu, I. D., Hitchiner, M. P., Uhlmann, E., Rowe, W. B., and Inasaki, I., 2006, Handbook of machining with grinding wheels, CRC Press.
[18] Linke, B. S., Corman, G. J., Dornfeld, D. A., and Tönissen, S., 2013, "Sustainability indicators for discrete manufacturing processes applied to grinding technology," Journal of Manufacturing Systems, 32(4), pp. 556-563.
[19] Zein, A., Li, W., Herrmann, C., and Kara, S., 2011, "Energy efficiency measures for the design and operation of machine tools: an axiomatic approach," Glocalized Solutions for Sustainability in Manufacturing, pp. 274-279.
[20] Rowe, W. B., 2013, Principles of modern grinding technology, William Andrew.
[21] Mohan, N., Ramachandra, A., and Kulkarni, S., 2005, "Influence of process parameters on cutting force and torque during drilling of glass–fiber polyester reinforced composites," Composite structures, 71(3-4), pp. 407-413.
[22] Chakraborty, S., Kar, S., Dey, V., and Ghosh, S. K., 2017, "Optimization and surface modification of al-6351 alloy using SiC–cu green compact electrode by electro discharge coating process," Surface Review and Letters, 24(01), p. 1750007.
[23] Das, J., and Linke, B., 2016, "Effect of Manual Grinding Operations on Surface Integrity," Procedia CIRP, 45, pp. 95-98.

Table 1: Behavioral differences based on operators inherent techniques

	Technique A	Technique B
Tool Velocity	Greater axial and less tangential	Less axial and more tangential
Gaze Frequency	More often	Less often
Gaze Shifts	More axial and less tangential	More tangential and less axial
Tangential Force	Lower	Higher
Surface Isotropy	Lower	Higher
Processing Time	Lower	Higher

Table 2: Quantitative analysis of behavioral differences of operators

	Technique A		Technique B	
Tool Velocity (m/sec)	**Axial (RMS)**	**Tangential (RMS)**	**Axial (RMS)**	**Tangential (RMS)**
	0.029	0.071	0.025	0.094
Gaze Frequency (Hz)	mean =1.26 SD =1.31		mean =0.86 SD =0.93	
Gaze Shifts (pixels)	**Axial (RMS)**	**Tangential (RMS)**	**Axial (RMS)**	**Tangential (RMS)**
	41.81	31.32	33.14	34.64
Tangential Force (N)	mean =5.17 SD =1.06		mean =7.07 SD =1.36	
Isotropy (%)	mean= 23.10, SD= 16.84		mean=39.38, SD= 26.72	
Processing Time (sec)	mean= 70.68, SD = 7.75		mean=81.50, SD = 20.68	

Table. 3: Optimal parameters for lower surface average roughness for all subjects

	Tangential Force (N)	Level	Normal Force (N)	Level	Depth of Cut (μm)	Level	Time (s)	Level
Subject 1	4	1	0.25	1	0.13	2	64	1
Subject 2	7	3	0.5	3	0.11	1	56.03	2
Subject 3	6	3	0.275	3	0.164	2	75	3
Subject 4	4.67	1	0.35	1	0.15	2	76.19	2

Table. 4. ANOVA Analysis based on Operator Technique

Subject 1 & 3			**Technique A**				
Machining Parameter	**Coefficient**	**Degrees of Freedom**	**Partial Sum of Squares**	**Mean Square**	**p Value**	**F Ratio**	**Contribution (%)**
Model		4	0.03	0.01		0.96	21.43
Tangential Force (F_t)	0.02	1	0.01	0.01	0.41	0.72	7.14
Normal Force (F_N)	-0.77	1	0.01	0.01	0.39	0.78	7.14
Depth of Cut (a_e)	0.22	1	0.001	0.001	0.75	0.1	0.71
Processing Time (t_p)	-0.01	1	0.03	0.03	0.08	3.58	21.43
Intercept	1.78	14	0.11	0.11			78.57
Total		18	0.14	0.01			

Subject 2 & 4			**Technique B**				
Machining Parameter	**Coefficient**	**Degrees of Freedom**	**Partial Sum of Squares**	**Mean Square**	**p Value**	**F Ratio**	**Contribution (%)**
Model		4	0.03	0.01		0.91	20
Tangential Force (F_T)	0.01	1	0.001	0.001	0.73	0.12	0.67
Normal Force (F_N)	-0.42	1	0.01	0.01	0.37	0.85	6.67
Depth of Cut (a_e)	-0.57	1	0.01	0.01	0.24	1.47	6.67
Processing Time (t_p)	0.001	1	0.01	0.01	0.38	0.81	6.67
Intercept	1.51	15	0.12				80
Total		19	0.15				

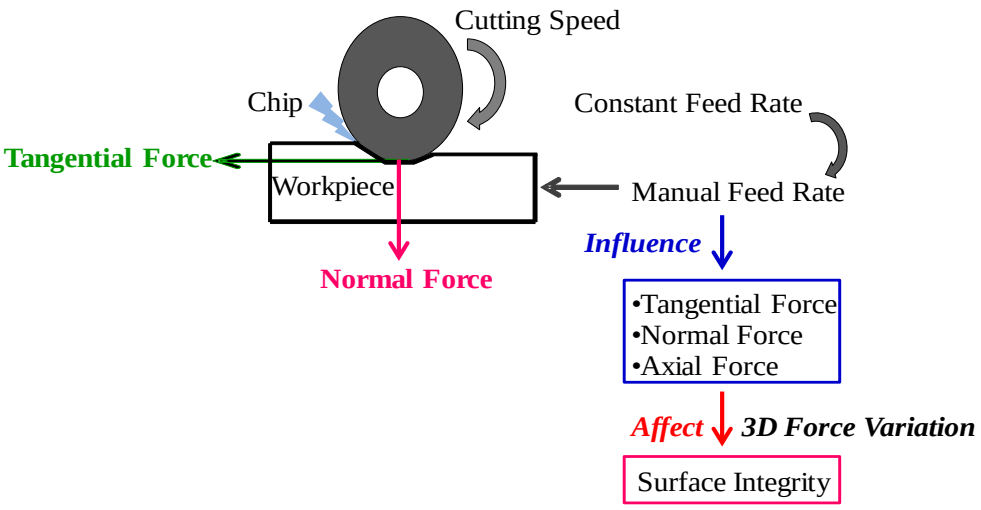

Fig. 1. Schematic of cutting force generation during manual grinding operation

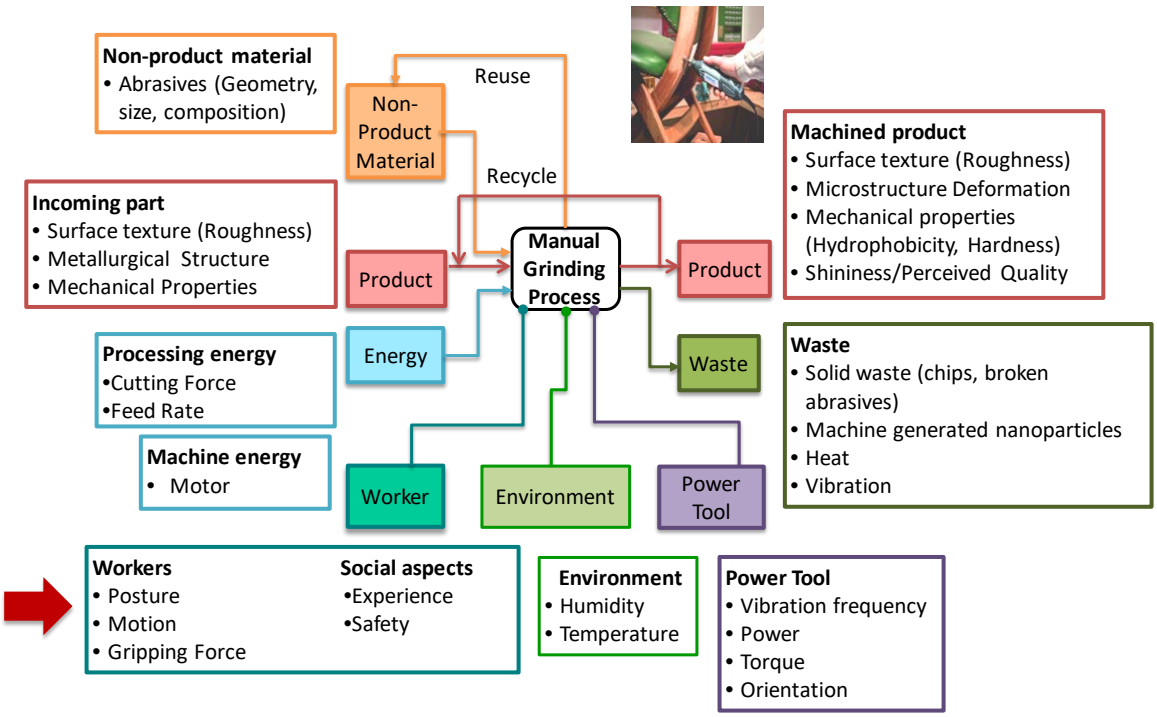

Fig. 2. Input-Output Diagram of Manual Grinding Process, reprinted from [23]

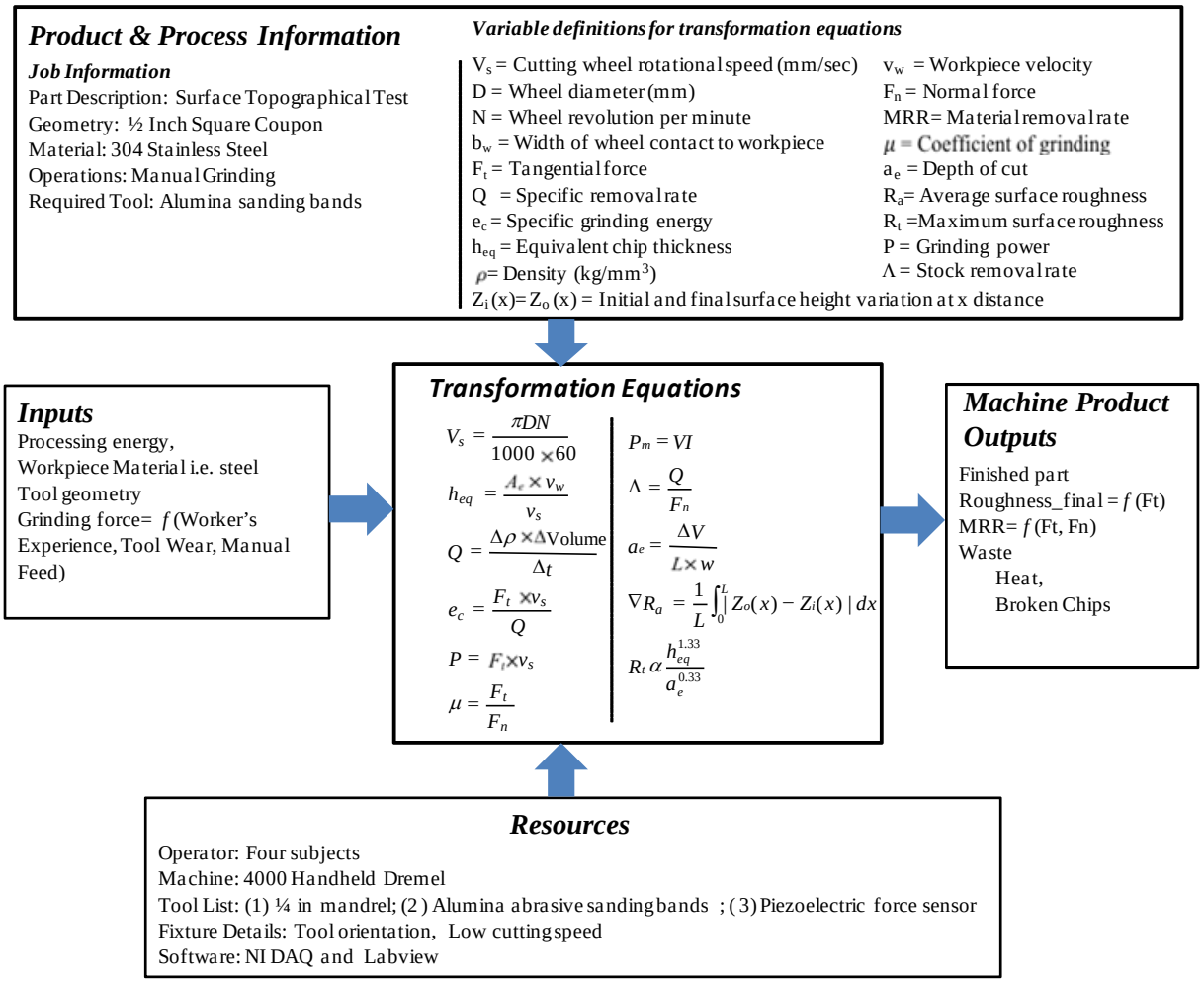

Fig. 3. Graphical representation of unit manufacturing process (UMP) for manual grinding operation

Fig. 4. Experimental Setup consists of eye tracking glasses, kinematic sensors, camera, and piezoelectric force sensor, reprinted from [4].

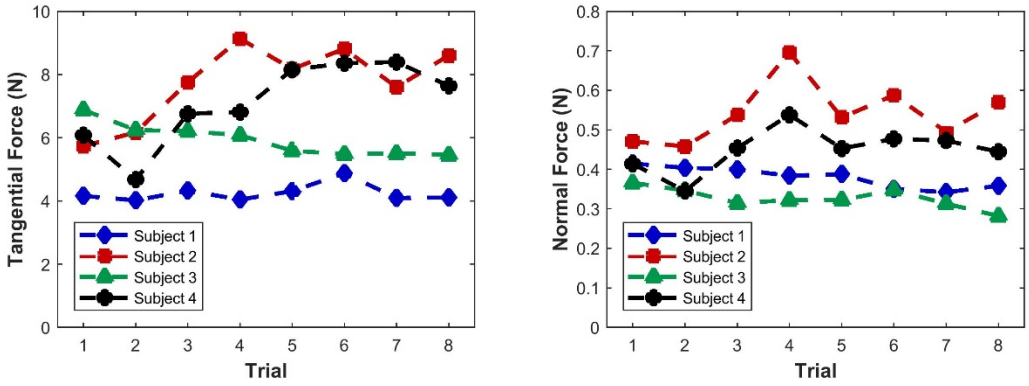

Fig. 5. Tangential and normal force for each subject

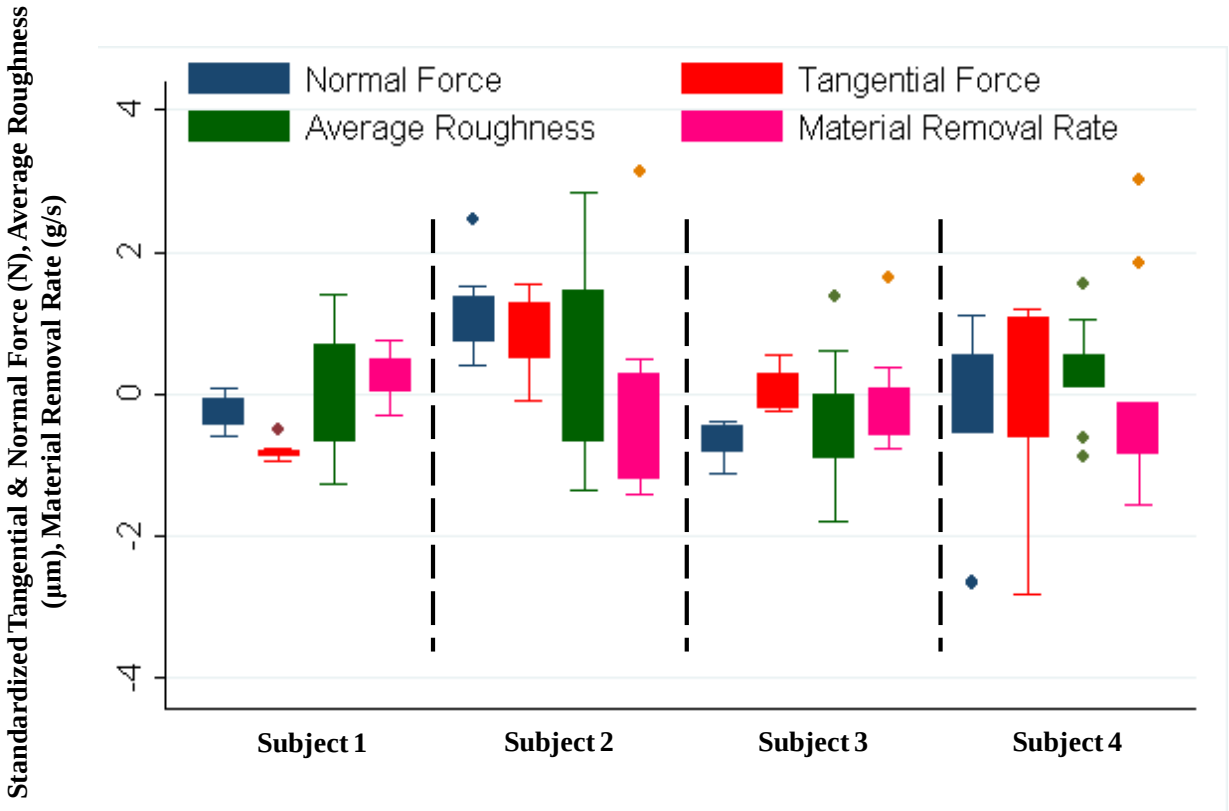

Fig. 6. Changes of average surface roughness and material removal rate with tangential and normalized normal force variation

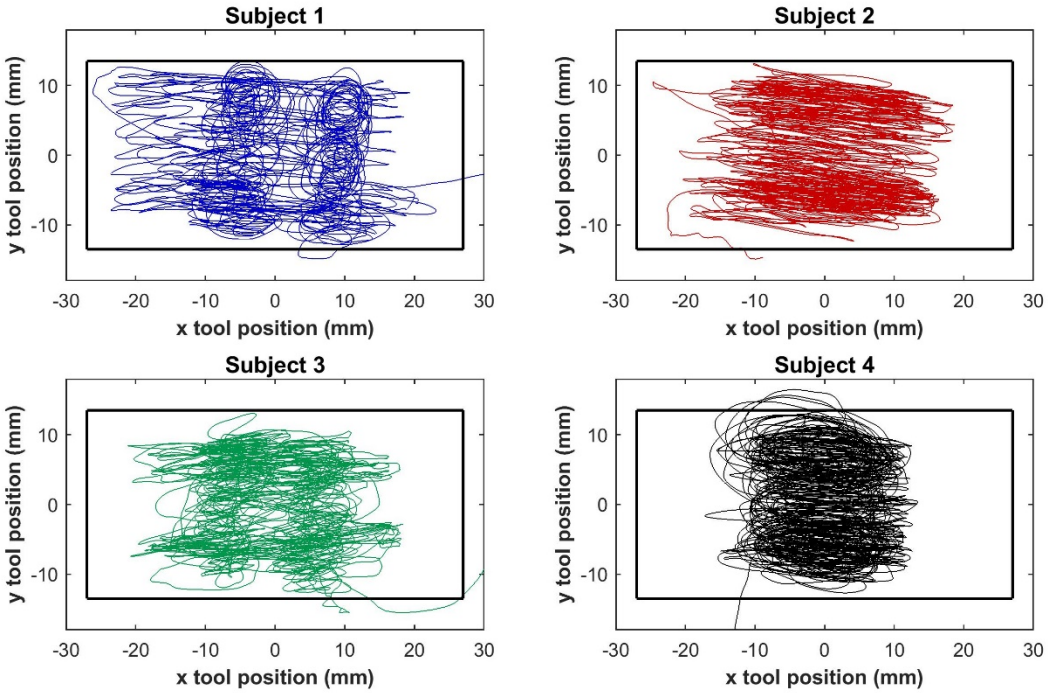

Fig. 7. Example grinding tool paths for each subject

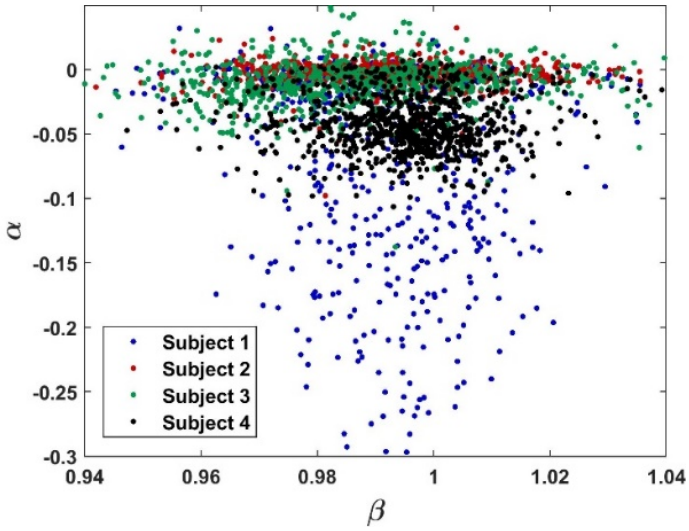

Fig. 8. Autoregressive parameters α and β for each subject for all ten trials

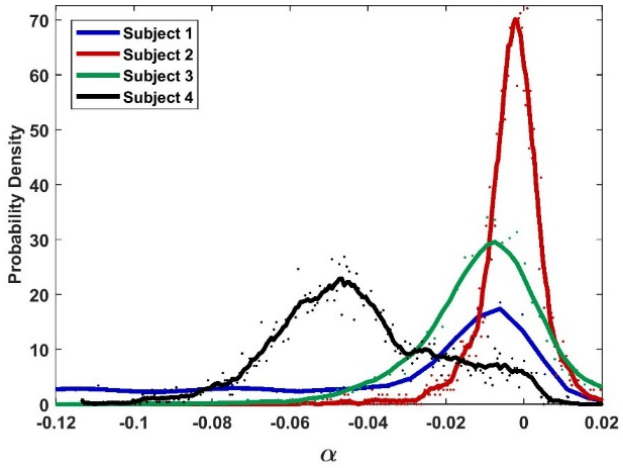

Fig. 9. Normalized histograms of the α parameter for all ten trials

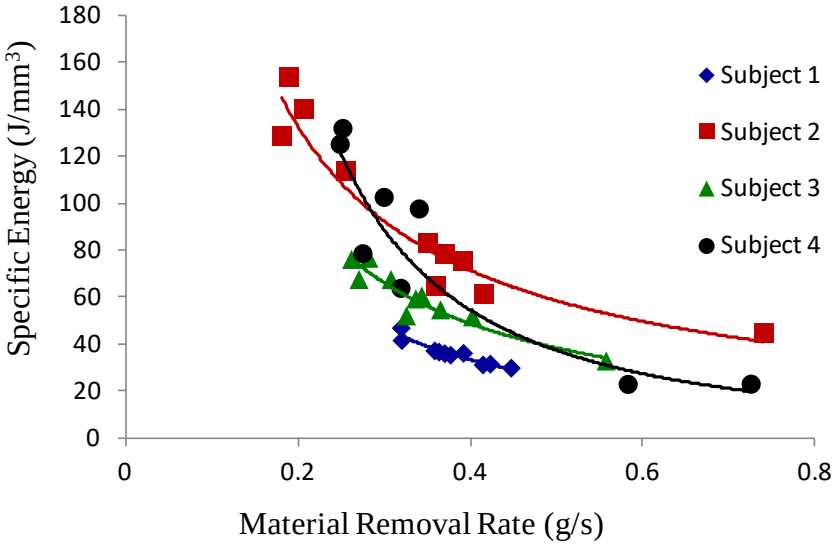

Fig.10. Specific energy consumption over material removal rate

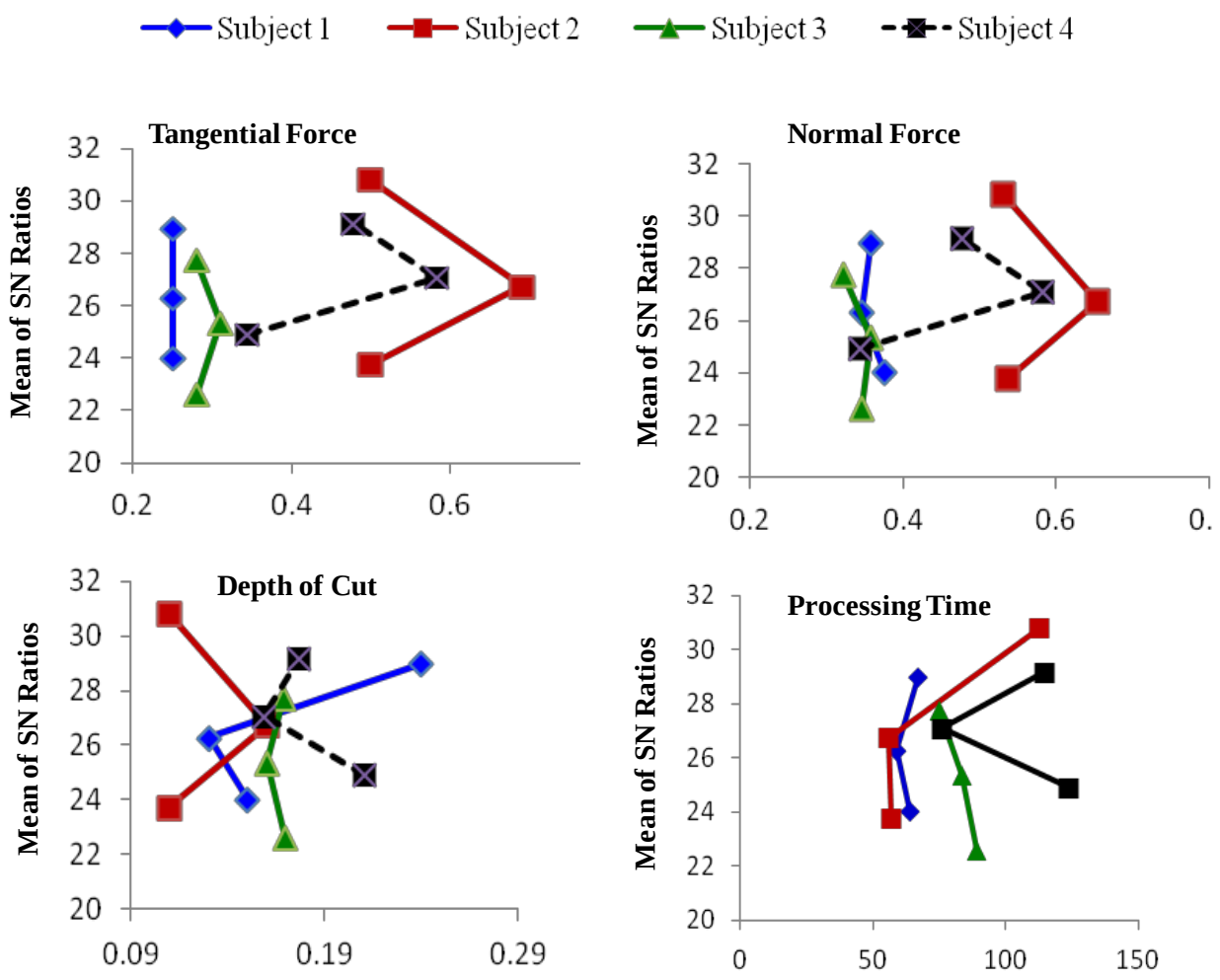

Fig. 11. Mean signal-to-noise (S/N) ratio graph for average surface roughness